Effects of density profile and multi-species target on laser-heated thermal-pressure-driven shock wave acceleration*

Wang Feng-Chao(王凤超)†

School of Science, Shanghai Institute of Technology, Shanghai 201418, *China*

(Received 19 April 2013; revised manuscript received 17 June 2013)

The shock wave acceleration of ions driven by laser-heated thermal pressure is studied through one-dimensional particle-in-cell simulation and analysis. The generation of high-energy mono-energetic protons in recent experiments (D. Haberberger *et al.*, 2012 *Nat. Phys.* **8** 95) is attributed to the use of exponentially decaying density profile of the plasma target. It does not only keep the shock velocity stable but also suppresses the normal target normal sheath acceleration. The effects of target composition are also examined, where a similar collective velocity of all ion species is demonstrated. The results also give some reference to future experiments of producing energetic heavy ions.

Keywords: laser–ion acceleration, shock wave, particle-in-cell simulation

PACS: 41.75.Jv, 52.38.Kd, 52.65.Rr **DOI:** 10.1088/1674-1056/22/12/124102

1. Introduction

High-energy proton or ion beams are very important for many significant applications, such as fast ignition fusion, cancer therapy, hadron colliders, etc.[1–3] Conventional accelerators usually require extraordinary occupying area and abundant cost because of the low accelerating gradient. These restrict their applications and popularizations. Plasma, however, could afford an electric field $4 \sim 5$ orders of magnitude higher than a conventional accelerator, thus becoming a promising medium for energetic proton/ion acceleration in a laboratory or even table-top size.

In most plasma-based accelerating schemes, ultra-intense laser pulses are used to drive strong electrostatic fields and accelerate protons/ions. The most familiar one is the target-normal sheath acceleration (TNSA),[4–11] where about 60-MeV protons have been produced with a 3×10^{20}-W/cm^2 laser.[6] The energy spread has also been reduced to about 20% using a micro-structured target.[9,10] Nevertheless the energy scaling law is quite weak, only about $E \sim \sqrt{I_0}$, where I_0 is the peak laser intensity, which makes it difficult to generate energy beyond hundred MeV. On the other hand, the light pressure acceleration (LPA) scheme[12–24] allows generating protons of GeV level with high efficiency. Great progress has been made in LPA theoretically. The experimental realization is limited by the instabilities developing during interaction. Recently, the proof-of-principle experiment obtained an about 30-MeV quasi-mono-energetic proton beam. People also proposed proton acceleration by plasma wakefield[25–28] in theory, which shows the potential of tens of GeV energy gain.

Another accelerating scheme is the collisionless shock wave acceleration (SWA).[29–36] The shock, normally stimulated by a linearly-polarized (LP) laser, carries a strong positive electrostatic field. When it propagates in plasma, some of the local protons can be trapped and reflected and finally have a constant velocity. The momentum conservation law indicates that the velocity of reflected protons is about twice the shock velocity. The high-energy proton beam from SWA is mono-energetic at the beginning. However, after they pass through the target normal sheath field, the spectrum is strongly expanded, which is very unfavorable for most applications.

Lately, an experiment showed that using a picosecond (ps) laser pulse from CO_2 system, proton beams with a peak energy of 20 MeV were produced, while the energy spread was as small as only a few percent. The results are quite surprising as the produced protons have much larger energy and lower energy spread than those predicted by the hole-boring shock.[31,32] This new scheme shows the prospect of producing 200-MeV protons with only a 10^{20}-W/cm^2 laser pulse. Unlike other mechanisms, it does not require an ultra-intense laser pulse so that it is more realizable to treat cancer in the near future.

In this paper, we study SWA in the above experiment. Through analysis and one-dimensional (1D) particle-in-cell (PIC) simulations, it is revealed that the shock is maintained by thermal pressure instead of the laser light pressure. The unexpected high energy comes from the large gradient of energy density, which is created by a target with exponentially decaying density distribution. The special density profile also suppresses normal TNSA to keep the proton beam mono-energetic.

*Project supported by the Shanghai Natural Special Foundation for Outstanding Young Teachers in University, China (Grant No. yyy10043).

†Corresponding author. E-mail: fcwang@sit.edu.cn

© 2013 Chinese Physical Society and IOP Publishing Ltd

2. Effect of density profile

We first introduce the simulation results with the code VORPAL.[37] The sketch is shown in Fig. 1, where a linearly-polarized laser is incident on a plasma target. The target density profile increases to maximum n_0 and remains constant within a length of l_0 and then decays exponentially to zero with $n = n_0 \mathrm{e}^{-x/l_{\mathrm{scale}}}$. In 1D PIC simulations, the laser pulse has a wavelength of $\lambda_0 = 0.8$ μm, peak amplitude of $a_0 = 10$, and pulse duration τ_0 of $20T_0$ (full width half maximum (FWHM)). Here T_0 is the laser period; $a = eE_0/m_{\mathrm{e}}\omega_0 c$ is the normalized laser field amplitude, where e and m_{e} are fundamental charge and electron mass respectively; E_0 and ω_0 are laser electric field and angular frequency respectively; c is the light speed. The simulation box is $300\lambda_0$ long with a resolution of 100 cells per wavelength. The maximum target density is $n_0 = 6n_{\mathrm{c}}$ with n_{c} being the critical plasma density and $l_0 = 2\lambda_0$. The target is located at $x = 20\lambda_0$. To see the effects of the exponential density profile, we change the length scale l_{scale} from 0 to $10\lambda_0$.

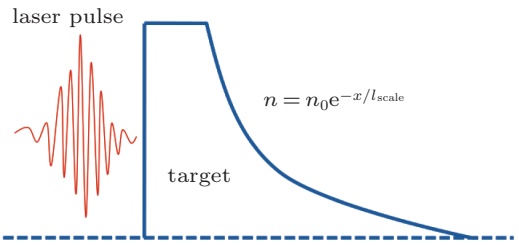


Fig. 1. (color online) Sketch of a relativistic laser pulse interacting with a density-decaying plasma target.

The simulation results are shown in Fig. 2. Distributions of proton momenta and the electron energy density are displayed for $l_{\mathrm{scale}} = 0$, $5\lambda_0$ and $10\lambda_0$ at the time of $300T_0$. For all three length scales, shocks are clearly formed at around $x = 40\lambda_0$. The incident laser pulse impinges on the target at about $20T_0$ and leaves the target at about $60T_0$. As seen in Fig. 2, the shocks propagate for a long time without laser pulses and local protons are continuously trapped and accelerated to quite a constant velocity. This demonstrates that unlike the case in the normal SWA, which is driven by the laser light pressure, these shocks are maintained by thermal pressure or electron energy density gradient. As one can see in Fig. 2, a clear energy density jump appears at the shock front in each case. In laser light-pressure driven SWA, the shock velocity is only determined by the laser field amplitude for certain ion species $v_s \sim a/\sqrt{n_0}$. One must increase the laser amplitude to obtain higher proton energy. However in thermal-pressure-driven SWA, the shock velocity is determined by electron temperature and the thermal pressure gradient. It then suggests that even with a relatively low-intensity laser pulse the shock velocity can be enhanced by designing some target structures to steepen the electron density gradient across the interface. That is why 20-MeV protons were obtained by using only a $a_0 \approx 2$ CO_2 laser in experiment, while in light-pressure SWA protons could only gain an energy of less than 1 MeV.

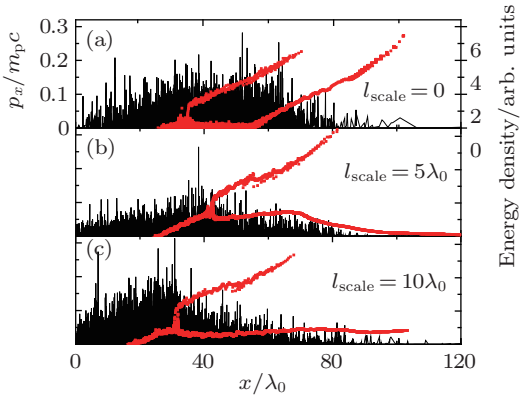


Fig. 2. (color online) Distributions of proton momentum p_x (red-dotted) and electron energy density (black solid) at the time of $300T_0$ for length scales of $l_{\mathrm{scale}} = 0$ (a), $5\lambda_0$ (b), and $10\lambda_0$ (c) respectively. The laser peak amplitude is $a_0 = 10$ and pulse duration is $\tau_0 = 20T_0$. The maximum target density is $n_0 = 6n_{\mathrm{c}}$.

In the experiments, the high energy density gradient is realized by using exponential decaying density profile. In Fig. 2 one notices that proton momenta are higher for the cases $l_{\mathrm{scale}} = 5\lambda_0$ and $10\lambda_0$. The most critical difference in momentum between with and without density ramp lies in the target normal sheath field. In Fig. 2(a), when the target density is uniform, the TNSA field peaks at the front of the expanding plasma and decays rapidly on both sides. As a result, protons located at the expanding front experience the most intense acceleration and achieve maximum energy, while the protons behind are accelerated less as shown in Fig. 3(a). When protons from the SWA propagate through the inhomogeneous TNSA field, the energy spectrum is greatly broadened, inducing an almost 100% energy spread. Furthermore, the shock velocity in uniform plasma decreases very fast. All these lead to a non-mono-energetic proton beam.

On the contrary, when the target has a density ramp, the TNSA field is uniformly distributed in the expanding region without an obvious peak as shown in Figs. 3(b) and 3(c). In such a manner, protons at the back of the target are uniformly accelerated. The phase space of TNSA protons shows a plateau profile as seen in Figs. 2(b) and 2(c). When protons accelerated by shock wave pass through the expanding plasma, they obtain a similar energy and thus keep the mono-energetic feature.

The exponentially decaying density profile also maintains the thermal pressure gradient for the shock wave. One could find in Figs. 2(b) and 2(c) that the electron energy density jump at the shock front is more obvious than in Fig. 2(a). This makes the shock velocity decay very slowly, thereby producing mono-energetic proton beams.

There is still a difference between with $l_{\mathrm{scale}} = 5\lambda_0$ and $10\lambda_0$. As can be seen in the corresponding phase space, the acceleration for $l_{\mathrm{scale}} = 10\lambda_0$ is more homogenous than for

$l_{\rm scale} = 5\lambda_0$, which would lead to a proton beam with less energy spread. It indicates that there should be an optimal density scale about the exponential decaying profile. This is related to electron cycling in the target. The efficient stimulation of a shock wave relies on homogeneously heated electrons, which can be achieved by electron recycling through the plasma target. For a certain target thickness of l, the time for electrons to pass through it is about l/c. To assure that electrons can recycle at least once during the interaction and be reheated by the laser pulse, the following requirement should be fulfilled:

$$\tau_0 > \frac{l}{c}, \tag{1}$$

which means that the target length scale should be smaller than the pulse longitudinal length. On the other hand, the suppression of normal TNSA requires a target length scale as large as possible, leading to an optimal foil thickness of about $l_{\rm opt} \sim c\tau_0$. In this case, the pulse duration is about $20T_0$, giving an optimal $l_{\rm scale}$ of about $10\lambda_0$. This is perfectly demonstrated in Fig. 3. The result of $l_{\rm scale} = 10\lambda_0$ offers both stable and mono-energetic proton acceleration.

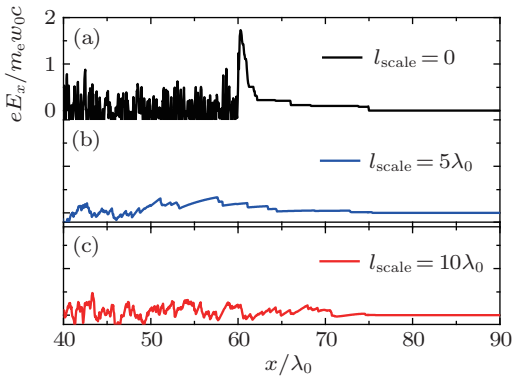


Fig. 3. (color online) Distributions of the electrostatic field at $t = 100T_0$ for length scales of $l_{\rm scale} = 0$ (a), $5\lambda_0$ (b), and $10\lambda_0$ (c) respectively. The laser-plasma parameters are the same as those in Fig. 2.

3. Effect of target composition

In this section, we perform a simulation study about the effect of target composition on thermal-pressure driven SWA. In the following 1D simulation, the laser parameters are the same as those in Fig. 2. The plasma targets have the same electron density profile. The targets contain two ion species, proton, and deuteron. We vary the density ratio between deuterons and protons $n_{\rm D}/n_{\rm H}$ to observe the momentum distributions of both ion species. Figure 4(a) shows the deuteron momenta for targets with only deuterons and $n_{\rm D}/n_{\rm H} = 10$, 1, and 0.1, respectively. As the proton fraction becomes more and more, the acceleration of deuterons becomes more unstable. Deuterons are not reflected continuously and they exhibit fractional structures in the phase space distribution.

The shock velocity and trapping field are determined by the charge-mass ratio of ion species. When the target contains more protons, the velocity will be higher and the trapping field smaller, which makes it more difficult to trap heavier ions, i.e., deuterons. Meanwhile, with more deuterons in the target, the shock will become slower and the field will become larger. Protons, with higher charge-mass ratio, are then more favorable to being accelerated.

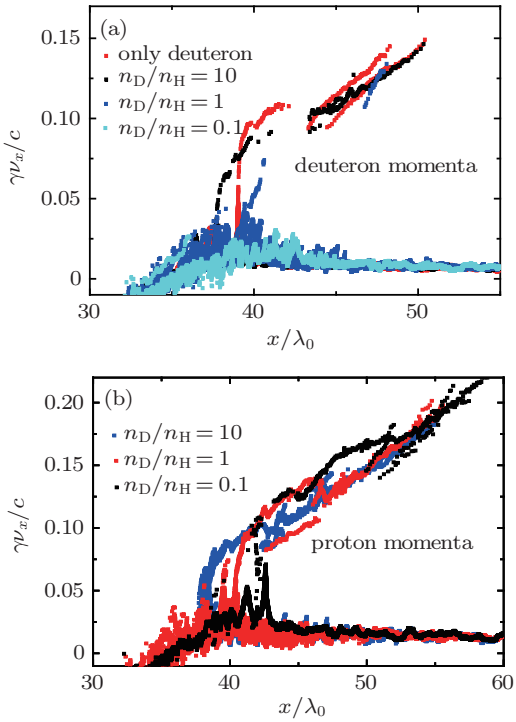


Fig. 4. (color online) Momentum distributions of deuterons (a) and protons (b) with $n_{\rm D}/n_{\rm H} = \infty$, 10, 1, and 0.1 at $t = 100T_0$, respectively.

The situation is quite different for protons as shown in Fig. 4(b). The shock velocity seems to increase with the increase of proton density and protons are well trapped and reflected in all cases. This is quite reasonable because a proton has higher charge-mass ratio and is more easily picked up by the shock. One important feature is that both ion species seem to move at a similar collective velocity, which is consistent with previous results,[38] where the electrostatic shock wave is driven by a circularly-polarized laser pulse. This is because both ion species belong to the same shock system, where only one shock velocity is allowed to exist. In such a case, protons are more easily trapped. They move faster than deuterons at first and then pass through the accelerating field in a shorter period, while deuterons move more slowly and experience a longer acceleration phase. As a result, they both obtain the same velocity.

However, when the deuterons are rare, say $n_{\rm D}/n_{\rm H} = 0.1$, they cannot be trapped anymore. Only protons are accelerated, leaving heavier deuterons that act as the background. This indicates that if heavy ions are the main concern, the target should not contain protons or other lighter ions with a high ratio. On the other hand, the acceleration of protons of

$n_D/n_H = 10$, i.e., in the deuteron-rich case, seems more constant and successive as shown in Fig. 4(b), which may open the way to better accelerating protons.

4. Conclusions

In this paper, ion acceleration by a thermal-pressure driven shock wave is examined. It is shown that the plasma density profile has an important influence on the shock velocity. An exponentially decaying density distribution leads to a stable acceleration and mono-energetic proton beam. The length scale of the density ramp is optimized. The effects of target composition are also studied. It is proved that both light and heavy ions are accelerated to the same collective velocity when they can be trapped and reflected. However, if one needs high-energy heavy ions, the light ion species should be eliminated.

References

[1] Roth M, Cowan T E, Key M H, Hatchett S P, Brown C, Fountain W, Johnson J, Pennington D M, Snavely R A, Wilks S C, Yasuike K, Ruhl H, Pegoraro F, Bulanov S V, Campbell E M, Perry M D and Powell H 2001 *Phys. Rev. Lett.* **86** 436

[2] Malekynia B and Razavipour S S 2013 *Chin. Phys. B* **22** 055202

[3] Malekynia B and Razavipour S S 2012 *Chin. Phys. B* **21** 125201

[4] Pukhov A 2001 *Phys. Rev. Lett.* **86** 3562

[5] Wilks S C, Langdon A B, Cowan T E, Roth M, Singh M, Hatchett S, Key M H, Pennington D, MacKinnon A and Snavely R A 2001 *Phys. Plasmas* **8** 542

[6] Snavely R A, Key M H, Hatchett S P, Gautier D C, Flippo K A, Letzring S, Johnson R P, Shimada T, Yin L, Albright B J, Bowers K J, Fernández J C, Rykovanov S G, Wu H C, Zepf M, Jung D, Liechtenstein V Kh, Schreiber J, Habs D and Hegelich B M 2000 *Phys. Rev. Lett.* **85** 2945

[7] Mora P 2003 *Phys. Rev. Lett.* **90** 185002

[8] Esirkepov T Zh, Bulanov S V, Nishihara K, Tajima T, Pegoraro F, Khoroshkov V S, Mima K, Daido H, Kato Y, Kitagawa Y, Nagai K and Sakabe S 2002 *Phys. Rev. Lett.* **89** 175003

[9] Schwoerer H, Pfotenhauer S, Jäckel O, Amthor K U, Liesfeld B, Ziegler W, Sauerbrey R, Ledingham K W D and Esirkepov T 2006 *Nature* **439** 445

[10] Hegelich B M, Albright B J, Cobble J, Flippo K, Letzring S, Paffett M, Ruhl H, Schreiber J, Schulze R K and Fernández J C 2006 *Nature* **439** 441

[11] Gaillard S A, Kluge T, Flippo K A, Bussmann M, Gall B, Lockard T, Geissel M, Offermann D T, Schollmeier M, Sentoku Y and Cowan T E 2011 *Phys. Plasmas* **18** 056710

[12] Macchi A, Cattani F, Liseykina T V and Cornolti F 2005 *Phys. Rev. Lett.* **94** 165003

[13] Ban H Y, Gu Y J, Kong Q, Li Y Y, Zhu Z and Kawata S 2011 *Chin. Phys. Lett.* **29** 035202

[14] Shen B F and Xu Z Z 2001 *Phys. Rev. E* **64** 056406

[15] Esirkepov T, Borghesi M, Bulanov S V, Mourou G and Tajima T 2004 *Phys. Rev. Lett.* **92** 175003

[16] Yan X Q, Lin C, Sheng Z M, Guo Z Y, Liu B C, Lu Y R, Fang J X and Chen J E 2008 *Phys. Rev. Lett.* **100** 135003

[17] Qiao B, Zepf M, Borghesi M and Geissler M 2009 *Phys. Rev. Lett.* **102** 145002

[18] Pegoraro F and Bulanov S V 2007 *Phys. Rev. Lett.* **99** 065002

[19] Zhang X M, Shen B F, Li X M, Jin Z Y and Wang F C 2007 *Phys. Plasmas* **14** 073101

[20] Robinson A P L, Zepf M, Kar S, Evans R G and Bellei C 2008 *New J. Phys.* **10** 013021

[21] Klimo O, Psikal J, Limpouch J and Tikhonchuk V T 2008 *Phys. Rev. ST Accel. Beams* **11** 031301

[22] Henig A, Kiefer D, Markey K, Gautier D C, Flippo K A, Letzring S, Johnson R P, Shimada T, Yin L, Albright B J, Bowers K J, Fernández J C, Rykovanov S G, Wu H C, Zepf M, Jung D, Liechtenstein V Kh, Schreiber J, Habs D and Hegelich B M 2009 *Phys. Rev. Lett.* **103** 045002

[23] Chen M, Pukhov A and Yu T P 2009 *Phys. Rev. Lett.* **103** 024801

[24] Yu T, Pukhov A, Shvets G and Chen M 2010 *Phys. Rev. Lett.* **105** 065002

[25] Shen B F, Zhang X M, Sheng Z M, Yu M Y and Cary J 2009 *Phys. Rev. ST Accel. Beams* **12** 121301

[26] Yu L L, Xu H, Wang W M, Sheng Z M, Shen B F, Yu W and Zhang J 2010 *New J. Phys.* **12** 045021

[27] Zhang X M, Shen B F, Ji L L, Wang F C, Wen M, Wang W P, Xu J C and Yu Y H 2010 *Phys. Plasmas* **17** 123102

[28] Zheng F L, Wang H Y, Yan X Q, Tajima T, Yu M Y and He X T 2012 *Phys. Plasmas* **19** 023111

[29] Denavit J 1992 *Phys. Rev. Lett.* **69** 3052

[30] Palmer C A J, Dover N P, Pogorelsky I, Babzien M, Dudnikova G I, Ispiriyan M, Polyanskiy M N, Schreiber J, Shkolnikov P, Yakimenko V and Najmudin Z 2011 *Phys. Rev. Lett.* **106** 014801

[31] Haberberger D, Tochitsky S, Fiuza F, Gong C, Fonseca R A, Silva L O, Mori W B and Joshi C 2012 *Nat. Phys.* **8** 95

[32] Fiuza F, Stockem A, Boella E, Fonseca R A, Silva L O, Haberberger D, Tochitsky S, Gong C, Mori W B and Joshi C 2012 *Phys. Rev. Lett.* **109** 215001

[33] Silva L O, Marti M, Davies J R, Fonseca R A, Ren C, Tsung F S and Mori W B 2004 *Phys. Rev. Lett.* **92** 015002

[34] Forslund D W and Shonk C R 1970 *Phys. Rev. Lett.* **25** 1699

[35] Forslund D W and Freidberg J P 1971 *Phys. Rev. Lett.* **27** 1189

[36] Romagnani L, Bulanov S V, Borghesi M, Audebert P, Gauthier J C, Löwenbrück K, Mackinnon A J, Patel P, Pretzler G, Toncian T and Willi O 2008 *Phys. Rev. Lett.* **101** 025004

[37] Nieter C and Cary J R 2004 *J. Comp. Phys.* **196** 448

[38] Ji L L, Shen B F, Zhang X M, Wang F C, Jin Z Y, Li X M, Wen M and Cary J R 2008 *Phys. Rev. Lett.* **101** 164802